

Article

Traction drive simulations when starting an electric locomotive series ŽS 444 on the railway tracks of Serbia

Branislav Gavrilovic^{1,*}, Vladimir Aleksandrovich Baboshin²

¹ Railway College, Academy of Technical and Art Applied Studies Belgrade, 11000 Belgrade, Serbia

² Department of Reconstruction of Automation, Telemechanics and Communication Devices on Railways, The Ulyanovsk Higher Military Command School of Communications, Sankt. Peterburg 198206, Russia

* **Corresponding author:** Branislav Gavrilovic, gavrilovic.branislav5@gmail.com

CITATION

Gavrilovic B, Baboshin VA. Traction drive simulations when starting an electric locomotive series ŽS 444 on the railway tracks of Serbia. *Mechanical Engineering Advances*. 2024; 2(2): 421.
<https://doi.org/10.59400/mea.v2i2.421>

ARTICLE INFO

Received: 5 July 2024

Accepted: 30 September 2024

Available online: 31 October 2024

COPYRIGHT



Copyright © 2024 by author(s).

Mechanical Engineering Advances is published by Academic Publishing Pte. Ltd. This work is licensed under the Creative Commons Attribution (CC BY) license.

<https://creativecommons.org/licenses/by/4.0/>

Abstract: The manuscript presents and describes the Model in Matlab-simulink, which allows to display the time change of the firing angle of the thyristor of the single-phase rectifier, the mean value of the voltage, the armature current and the speed of the electric motor during the start-up of the electric locomotive ŽS 444 series for different given mechanically loaded and reference speeds of traction electric motors. The model makes it possible to establish the desired reference speed change ramps for different reference speeds and mechanical loads from +250 rpm, i.e., the maximum current of the electric motor armature up to 1250 A.

Keywords: railways of Serbia; electric locomotive ŽS 444 series; direct current electric motor

1. Introduction

Electric locomotives of the 444 series, known as “Severine”, were obtained by improving 30 electric locomotives of the 441 series. Improvements are reflected in the application of thyristor converters, which enabled the continuous regulation of traction motor current. The drive is divided into two independent twin-engine units. Certain improvements have also been made in the functioning of the electrodynamic (electro resistive) brake. The new system of regulation of the locomotive’s electric motor drive was realized with the help of a microprocessor. In general, there was not much modernization in the mechanical part. After the reconstruction and modernization of 30 locomotives, the 441 series was renumbered to 444 (from 001 to 030) and was put into traffic during the following years (2004–2007).

The designer of this type is ASEA from Sweden, and the license for the production of these locomotives was taken over by the Croatian factory “Rade Končar” in 1970 in cooperation with “MIN” from Niš, Serbia [1–3].

Figure 1 shows the layout, and **Figure 2** shows a simplified diagram of the ŽS 444 series electric locomotive.



Figure 1. Appearance of the ŽS 444 series electric locomotive [4].

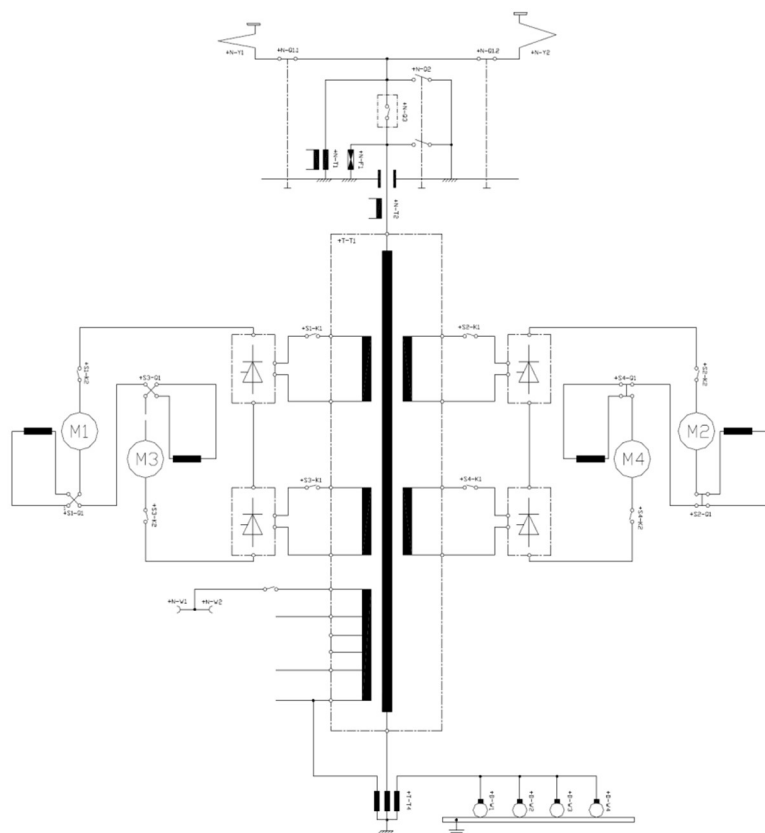


Figure 2. Simplified diagram of the main circuit in traction [4].

Table 1 shows the basic data of the ŽS 444 series electric locomotive [4].

Table 1. Technical data of the electric locomotive series ŽS 444 [4].

| Parameter | The data |
|---|-------------|
| Axle arrangement | Bo' Bo' |
| Track width | 1.435 mm |
| The distance between the axles in the stand | 2.700 mm |
| Pedestal spacing | 7.700 mm |
| Total mass of locomotives | 78 t ± 2 % |
| Axle pressure | 19.5 t ± 2% |

Table 1. (Continued).

| Parameter | The data |
|---|------------|
| Top speed | 120 km/h |
| Transmission ratio of the axle gear | 1 : 3, 65 |
| Lasting power | 3.860 kW |
| Maximum traction | 276 kN |
| One-hour traction | 188 kN |
| Permanent traction | 175 kN |
| Power for electric heating | 800 kVA |
| Contact network voltage | 25 kV |
| The highest height of the contact line | 6.500 mm |
| Temperature range of locomotive operation | -25–+40 °C |

2. Locomotive model in Matlab-Simulink

2.1. Modeling and simulation methodology

In general, the simulation of complex systems such as electric locomotives of the ŽS 444 series helps to understand those systems and has an indispensable role, considering that experimenting with this system is often impossible, impractical, too expensive, time-consuming and too dangerous.

Modeling and simulation of the ŽS 444 series electric locomotive (which are often considered together, as compatible techniques that have the same goal), were carried out in the following three stages.

- Task setting

Before starting the act of modeling and simulation, the tasks and goals of the research are clearly defined. These findings were reflected in the need for a clear understanding of the dynamic state of operation of the devices and equipment of the main circuit immediately when the locomotive of the ŽS 444 series was started. In doing so, it was insisted on understanding first of all: temporal changes in the firing angle of the thyristor of the single-phase rectifier, the mean value of the voltage, the armature current and movement speed. of the electric motor when starting the electric locomotive for different mechanical loads of the locomotive. In view of the need for the smallest possible degree of idealization (approximation) of locomotive operation, the simulation model in Matlab-Simulink was chosen, this is because Matlab-Simulink offers three options for describing the ŽS 444 series locomotive that can be combined: locomotive description using higher programming languages, locomotive description using Matlab functions and graphical representation of the model using blocks. At the same time, using blocks is the most convenient and fastest way to edit the model until the desired results are achieved [4].

- Studying the system and forming a structural scheme

After setting the task and defining the stated goals, we started identifying and determining the limits of the System (technical characteristics of the locomotive), as well as its components and the way they interact. The variable quantities, their arrangement and mutual relations, as well as the inputs and outputs of the system, are defined. At the same time, the change in contact network voltage was defined as a

possible external influence on the proper operation of the locomotive. The ranges of possible changes in this voltage are determined within the limits of 19 kV to 27.5 kV.

- Model development

The simulation of electric locomotives of the ŽS 444 series in principle boils down to determining the behavior of the model based on the set input values (voltage of the contact network, set limit speed of movement and mechanical load of the locomotive). With this simulation, the accuracy of the model was evaluated by comparing the values of individual variables in the process and the corresponding values of the variables in the model. The results of the simulations were continuously analyzed during the creation of the model with the necessary evaluation of the model until the results were not satisfactory with the experimental results that were available.

2.2. Structural scheme of the model

Figure 3 shows the model of the 444 series electric locomotive in Matlab-Simulink during speed control. The model illustrates a single-phase thyristor converter drive used to power an 850 kW DC motor. The locomotive’s thyristor converters are fed to the 25 kV, 50Hz catenary via the main transformer to step down the voltage to 1265V (no-load). The technical characteristics of the main transformer are given in **Table 2** [4].

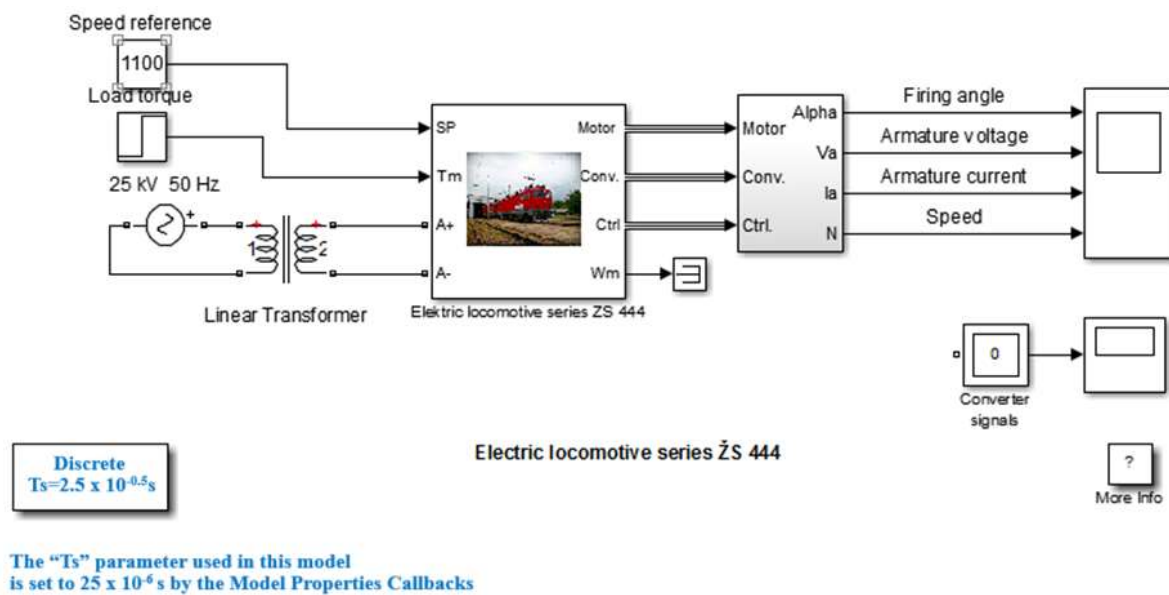


Figure 3. Structural scheme of the model of the 444 series electric locomotive in Matlab-Simulink during speed control.

The locomotive model is built from five main blocks. The DC drive electric motor, single-phase thyristor rectifier and thyristor bridge firing unit blocks are provided from the SimPowerSystems™ library while the speed controller and traction motor current controller blocks are specific and modeled separately. The armature voltage of the motor is provided by a two-square thyristor rectifier controlled by PI current and speed regulators through the main choke of inductance 4.5 mH. The speed controller provides the armature current reference (in pu) through the speed sensor, which is used by the current controller to obtain the electromagnetic torque required

to achieve the desired speed. The rate of change of the speed reference follows the acceleration and deceleration ramps to avoid sudden reference changes that could cause excessive armature current and destabilize the system. The current regulator controls the armature current by calculating the appropriate firing angle of the thyristor. This generates the rectifier output voltage required to obtain the desired armature current. The block “regulation switch” allows switching from one type of regulation to another. During current (torque) regulation, the speed controller is disabled. **Figure 4** shows the model of the locomotive at speed regulation with the above blocks.

Table 2. Technical characteristics of the main electrical transformer series 444 [4].

| | |
|--|--|
| Nominal primary voltage | 25 kV, 50 Hz |
| The highest voltage of the traction secondary (no load) | 1265 V |
| Voltage for electrodynamic braking in end position | 115 V |
| Train heating voltage (idle) | 1525 V |
| Permanent train heating current | 335 A (max 400A) |
| Voltages on the outputs of the secondary for the auxiliary drive | 403 V, 482 V (546V), 718 V, 892 V (1009 V) |
| Secondary traction power | 4 × 1265 kVA |
| Secondary power for auxiliary drive | 115 kVA |
| Cooling | OFAF (forced oil, forced air) |

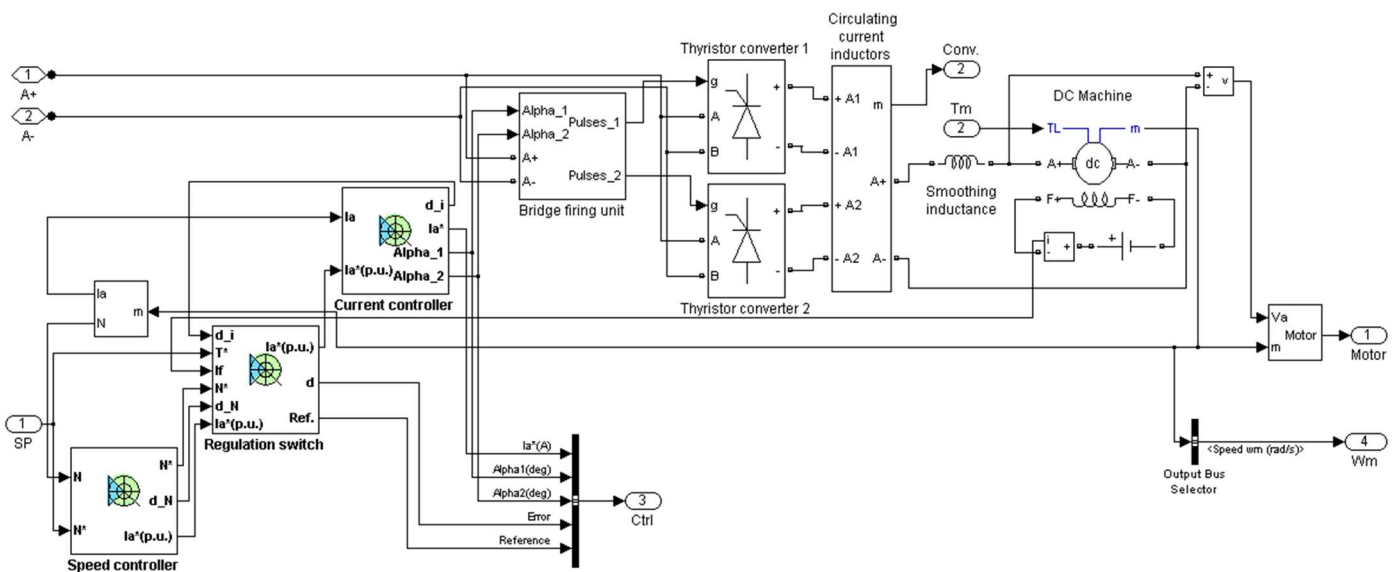


Figure 4. Blocks as integral parts of the ŽS 444 series electric locomotive.

2.3. Speed regulator block

The speed controller is shown in **Figure 5** and uses a PI controller. The controller provides an armature current reference (in pu) that is used by the current regulator to obtain the electromagnetic torque required to achieve the desired speed. During torque regulation, the speed controller is disabled [5–7].

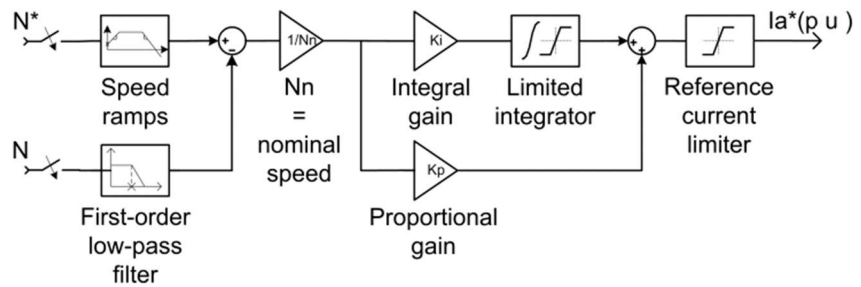


Figure 5. Traction electric motor speed regulator block.

The speed controller takes the speed reference (in rpm) and the rotor speed of the DC traction electric motor as input parameters. The rate of change of the reference speed will follow the acceleration and deceleration ramps that are predefined to avoid sudden reference changes that could cause excessive armature current and destabilize the system. The velocity measurement is filtered using a first-order low-pass filter. The current reference output is limited between 0 pu and a predefined upper limit.

2.4. Current regulator block

The armature current regulator is shown in **Figure 6** and uses a second PI controller. The regulator controls the armature current by calculating the appropriate firing angle of the thyristor. This generates the rectifier output voltage required to obtain the desired armature current and thus the desired electromagnetic torque. The controller takes the current reference (in pu) and the armature current flowing through the motor as input parameters. The current reference is either provided by the speed controller during speed control or is calculated from the torque reference that is preset during torque control. This is controlled by means of a block: “control switch” [5,8,9].

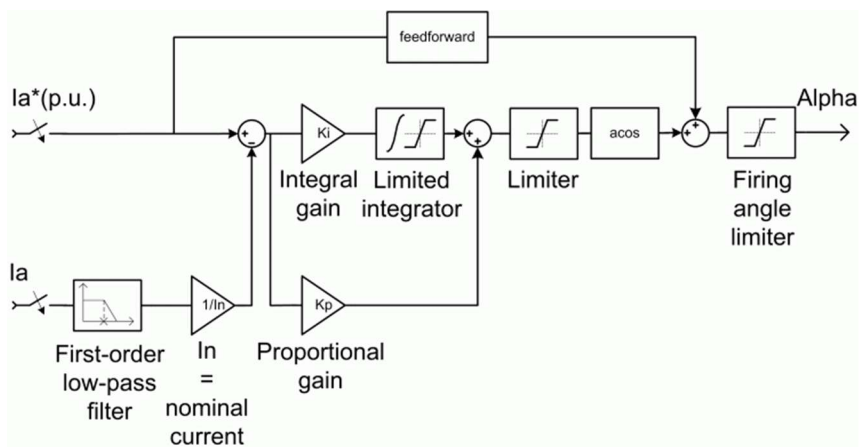


Figure 6. Traction electric motor armature current regulator block.

The armature current input is filtered using a first-order low-pass filter. The arcsin function is used to linearize the control system during continuous execution. To compensate for the nonlinearities that appear during discontinuous conduction, the firing angle is added in advance. This improves system response time. The shooting angle can vary between 0 and 180 degrees.

2.5. Single-phase thyristor rectifier block

The thyristor rectifier block consists of one controlled current source on the AC side and one controlled voltage source on the DC side (Figure 7) [5,10–26].

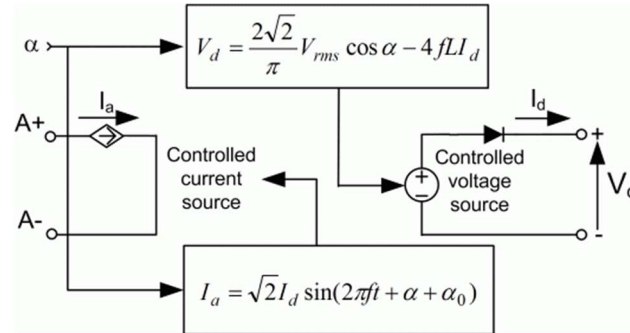


Figure 7. Single-phase thyristor rectifier block.

The input, alternating current of the rectifier is given by the following equation:

$$I_a = \sqrt{2}I_d \sin(2\pi ft + \alpha + \alpha_0) \quad (1)$$

where are they:

α —ignition angle value,

α_0 —phase angle on the alternating current side,

f —alternating current frequency i ,

I_d —value of the rectified output current.

The DC output voltage of the rectifier represents the average value of the rectified voltage waveform for the continuous armature current according to the following equation:

$$V_a = \frac{2\sqrt{2}}{\pi} V_{rms} \cos \alpha - 4fLI_d \quad (2)$$

where are they:

V_{rms} —input rms voltage value, and

L —source inductance.

2.6. The pulse generator block for starting the thyristor rectifier

The discrete synchronized pulse generator block generates pulses for firing the rectifier thyristors. The Synchronized 6-Pulse Generator block is configured to operate in double-pulse mode. In this mode, two pulses are sent to each thyristor: the first pulse when the alpha angle is reached, then the second pulse 60 degrees later, when the next thyristor is activated.

Figure 8 shows six-pulse synchronization for an alpha angle of 30 degrees and with a dual-pulse mode. It is easy to see that the pulses are generated 30 degrees after the zero crossing between line to line [12–14].

The sequence of pulses at the output of the block corresponds to the natural sequence of commutation of the three-phase thyristor bridge. When a 6-pulse synchronized generator block is connected to the pulse input of a universal bridge block (with thyristors as a power electronic device), the pulses are sent to the thyristors

in the following order [12,15–26]:

- Input alpha 1 is an alpha signal in degrees and is connected to the controller system for controlling the pulse of the generator, a
- Inputs alpha 1, A+ and A-AB are the inputs to which the synchronization voltage is supplied, which is in phase with the input AC voltage of the single-phase thyristor rectifier.
- Input 5 allows the operation of the generator to be blocked. The output contains two pulse signals.

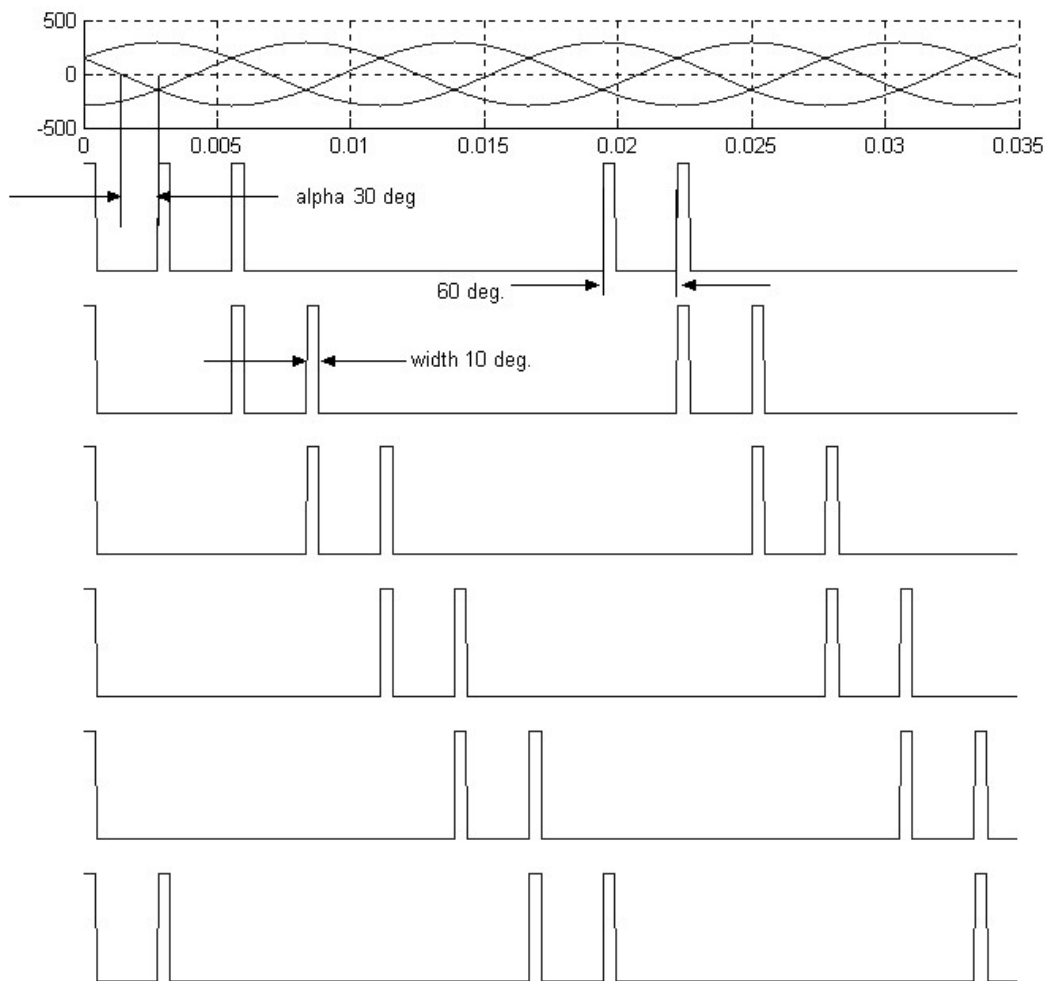


Figure 8. Synchronized 6-pulse generator block configured in dual-pulse mode.

3. Locomotive table dialog

The dialogue box of the locomotive consists of: the dialogue table of the drive electric motor, thyristor rectifier and controller.

3.1. Drive electric motor table dialog

Traction electric motors of locomotives are unidirectional wave machines of different types LJE 108-2 (ASEA, ELIN, ELECTROPUTERE) and ISVK 644-8 (KONČAR), but of exactly the same construction, identical parameters and

characteristics. The technical characteristics of the electric motor are given in **Table 3** [2–4].

Table 3. Nominal data of traction motors of the ŽS 444 series locomotive.

| | Permanently | One hour | Maximum |
|----------------------|-------------|----------|---------|
| Voltage (V) | 770 | 770 | 870 |
| Current (A) | 1180 | 1250 | 1715 |
| Rotation speed (rpm) | 1100 | 1185 | 1715 |
| Power (kW) | 850 | 900 | |
| Full Excitation (%) | 87 | | |
| Min. Excitation (%) | 45 | | |

The drive electric motor dialog table is shown in **Figure 9** and provides the electrical parameters and mechanical parameters of the motor. The electrical parameters of the motor refer to the ohmic and inductive resistance of the windings of the stator and rotor of the motor. Given that a speed of 1100 (rpm) was chosen as the mechanical input when modeling the mechanical system of the engine, the electromagnetic torque as an output quantity was obtained based on the expression:

$$T_e = J \frac{d}{dt} \omega_r + F \omega_r + T_m \quad (3)$$

where are they:

- J —coefficient of inertia of all rotating masses of the engine ($J = 0.25 \text{ kg m}^2$),
- F —coefficient of viscous friction.
- T_m —coefficient of torsional friction.

During the conducted simulations, it was assumed that: $J = 0.25 \text{ kg m}^2$, $F = 0.01 \text{ Nms}$, $T_m = 0.01 \text{ Nm}$ [2–4].

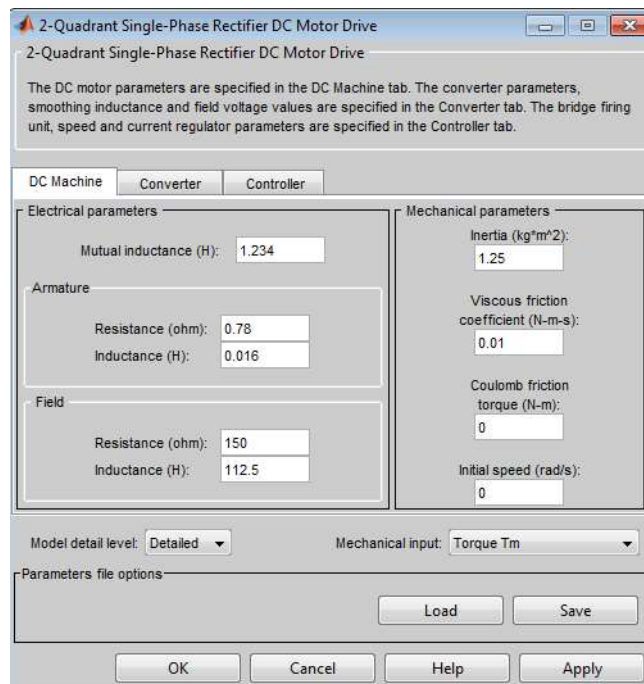


Figure 9. Layout of the dialog table of the drive electric motor of direct current.

3.2. Thyristor rectifier table dialog

Value of voltage and inductance of the excitation winding of the motor, value of single-phase voltage and inductance of the source connected to the A+, A- block of the pulse generator for firing the thyristor rectifier are shown in **Figure 10**.

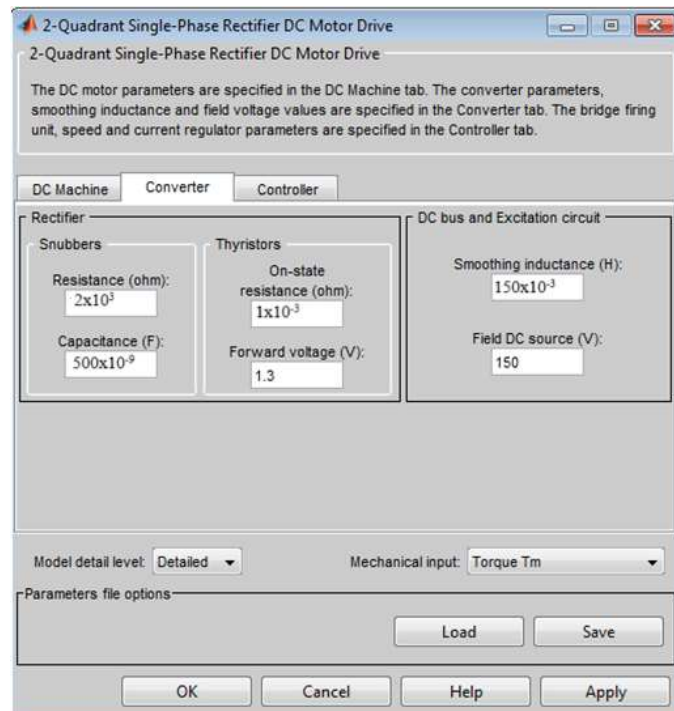


Figure 10. Layout of the thyristor rectifier table dialog.

3.3. Controller table dialog

The controller table dialog gives the possibility to select the parameters of the speed controller, the current controller and the thyristor bridge firing unit.

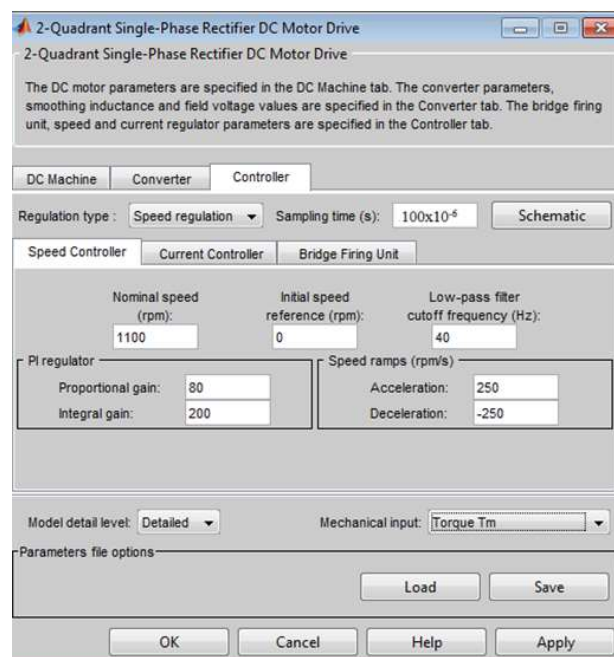


Figure 11. Layout of the speed controller table dialog.

A dialog of the table and relevant values of the speed controller parameters is given in **Figure 11**.

The current controller table and parameters dialog is given in **Figure 12**.

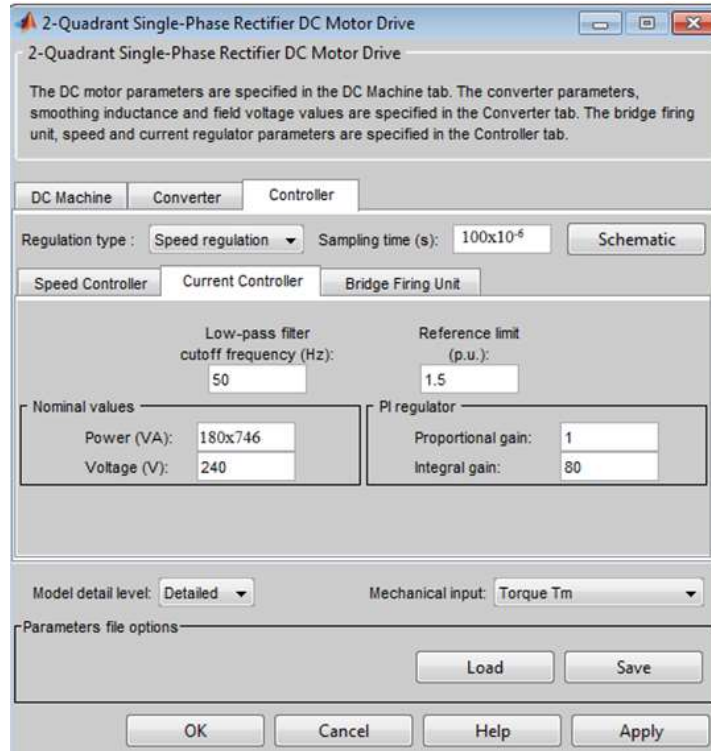


Figure 12. Layout of the current controller table dialog.

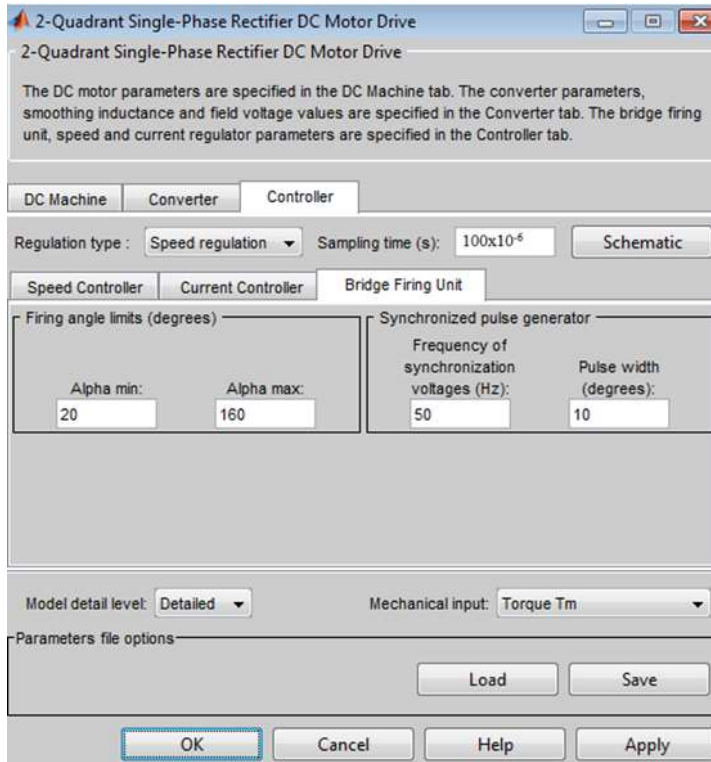


Figure 13. Layout of the thyristor bridge ignition unit dialog.

The layout of the dialog table and relevant parameters of the thyristor bridge firing unit controller is given in **Figure 13**.

4. Results of simulations

Figures 14 and 15 show the results of simulations of the change in firing angle of the rectifier thyristor, voltage and armature current, and at the set reference speed of 1100 rpm at the moment $t = 0$ s of the electric motor. In both simulations, an initial torque on the electric motor shaft of 15 N m was assumed.

The speed of the electric motor in both cases follows the reference ramp (+250 rpm) and reaches a stable state around $t = 8.75$ s when the load moment in the first case goes from 15 N.m. to 20 N.m. (light passenger trains), and in the second case from 15 N.m. to 100 N.m. (heavy freight trains).

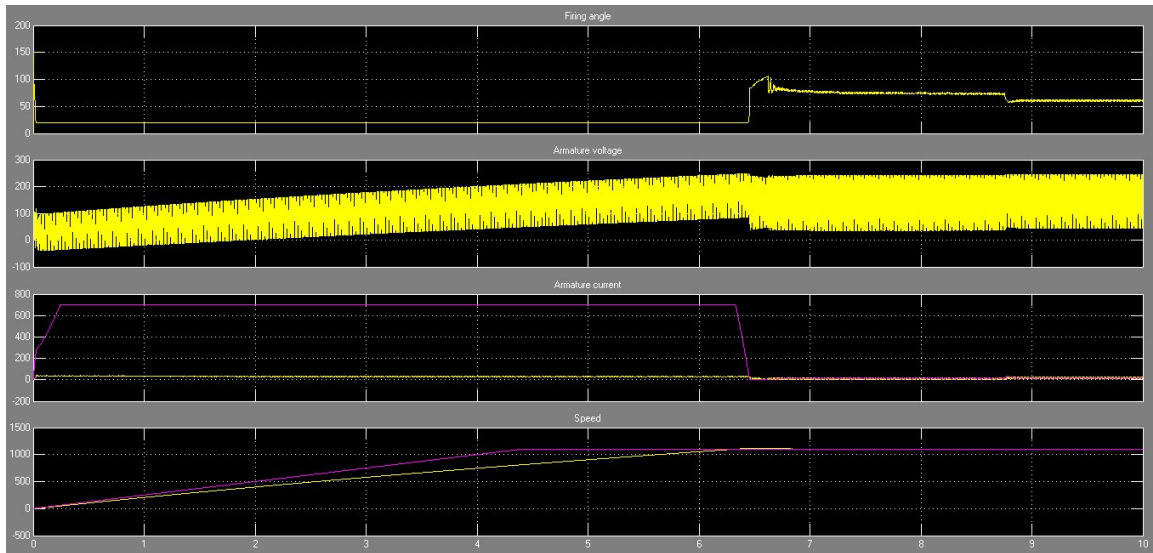


Figure 14. Temporal changes of the ignition angle of the rectifier thyristor, voltage and armature current of the ŽS 444 series locomotive electric motor in light passenger trains.

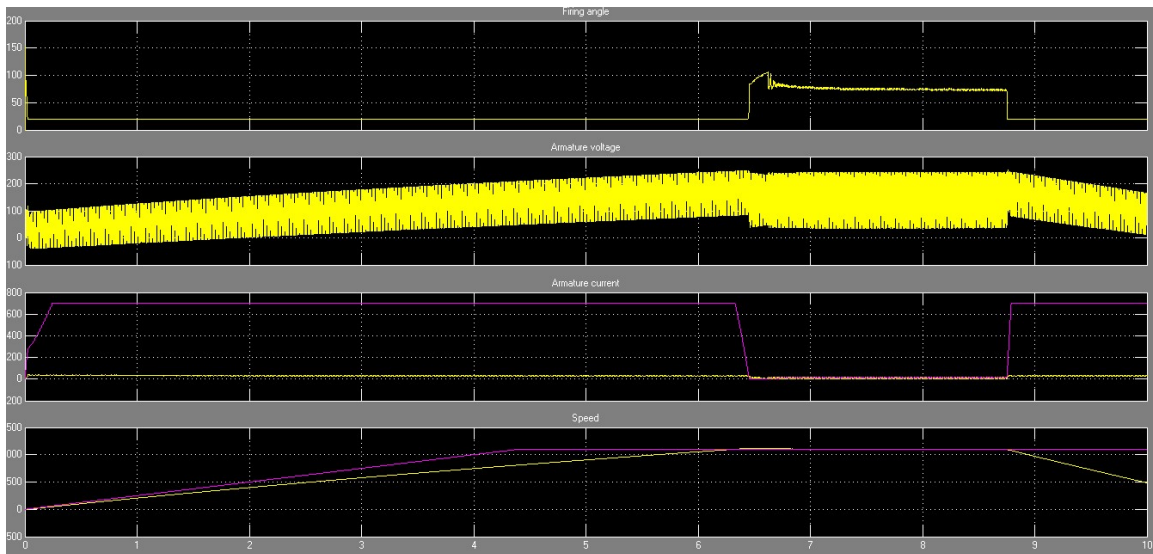


Figure 15. Temporal changes of the ignition angle of the rectifier thyristor, voltage and armature current of the ŽS 444 locomotive electric motor in heavy freight trains.

The armature current follows the reference current very well in both cases, and the firing angle remains at the lower limit of 20 degrees until $t = 6.35$ s after which it takes on higher values, still below 90 degrees to keep the converter in rectifier mode (first mode quadrant). The mean value of the armature voltage of 240V was reached in $t > 6.35$ s.

In both analyzed cases, the engine speed increases rapidly and recovers to 1100 rpm at $t = 10$ s. When the engine starts (starting the locomotive), the armature current in both cases increases to 720 A, but at the moment $t = 6.35$ s and reaches the nominal speed, the current in both cases drops to a significantly lower value of 10A. In the first case, such a low value of the armature current remains unchanged for $t > 8.75$ s, while in the second case, it rises again to 720A at that moment due to a significantly higher load on the electric motor and the need for a higher electromagnetic torque to maintain the required speed. The armature current perfectly follows its reference value, which in this case is set to 730 A.

5. Discussion

The simulation model of the locomotive ŽS 444 series in Matlab-Simulink, described in chapter 2 of this manuscript, enables a clear visualization of the following output values: temporal changes in the firing angle of the single-phase rectifier thyristor, mean voltage values, armature current and movement speed. traction electric motors when starting an electric locomotive for different mechanical loads of the locomotive. This possibility was achieved by taking into account the technical characteristics, arrangement and mutual influence of all devices in the main circuit of the locomotive as described in chapter 3 of this manuscript. Two physical quantities appear as input to the realized system: the contact network voltage and the mechanical load of traction electric motors. Therefore, it can be said that the realized model allows not only to see the sensitivity of the above-mentioned output values, but also their dependence for different mechanical loads of traction electric motors.

The following results were obtained when the locomotive was started from rest and at a set nominal voltage of the contact network of 25 kV and a mechanical load of the traction electric motors of 15 N.m. (light passenger trains) or 100 N.m. (heavy freight trains):

- The armature current follows very well the reference current of 730 A in both cases, and the firing angle remains at the lower limit of 20 degrees until $t = 6.35$ s after which it takes on higher values, still below 90 degrees to keep the converter in mode rectifier (first mode quadrant). The mean value of the armature voltage of 240 V was reached for $t > 6.35$ s.
- At the set reference speed of 1100 rpm at the moment $t = 0$ s, the speed of the electric motor in both cases follows the reference ramp (+250 rpm) and reaches a steady state around $t = 8.75$ s.
- - In both analyzed cases, the engine speed increases rapidly and returns to the set reference speed of 1100 rpm at $t = 10$ s. When starting the engine (starting the locomotive), the armature current in both cases increases to 720 A, but at the moment $t = 6.35$ s and reaching the rated speed, the current in both cases drops to a significantly lower value of 10 A. In the first case, such a low value of the

armature current remains unchanged $t > 8.75$ s, while in the second case it increases again to 720 A at that moment due to a significantly higher load on the electric motor and the need for a higher electromagnetic torque to maintain the required speed. The armature current perfectly follows its reference value, which in this case is set to 730 A.

The above results indicate a fast and efficient automatic regulation of the locomotive speed and traction electric motor current when starting light (passenger) and heavy (freight) trains.

In addition to the observed examples, it is also possible to observe the time change of the specified output values for other values of the resistance moment and voltage of the contact network. In the simulations that were carried out at different contact network voltages from 19 kV to 27.5 kV. and at the same mechanical loads of 15 Nm and 100 Nm they show almost the same results as at a voltage of 25 kV. This fact indicates an important characteristic of the locomotive, i.e., that the locomotive drive is not sensitive to permitted changes in the contact network voltage.

The above simulation results were experimentally confirmed based on numerous measurements carried out on these locomotives [4].

6. Conclusion

For different mechanically loaded and reference rotation speeds of the traction electric motors of the electric locomotive ŽS 444 series, the model provides a clear picture of the time change of the thyristor firing angle of the single-phase rectifier, the mean value of the voltage, the armature current and the rotation speed of the electric motor when the locomotive starts up.

When starting the locomotive, the mean value of the armature current of the electric motor does not exceed the set value (720 A). This value can be adjusted up to 1250 A (one-hour permissible value of the electric motor) if adhesion conditions between the wheel and the rail of the locomotive allow it. At higher mechanical loads, this value is retained longer due to the need for higher electromagnetic torques at higher speeds. Regardless of the value of the set reference armature current, the armature current during the starting of the electric motor always follows it perfectly.

In addition to the set speed reference value of 1100 rpm and the initial mechanical load of 15 Nm, i.e., the load of 20 Nm and 100 Nm after $t = 8.75$ s, other speed reference values and the mechanical load of the electric motor can be set, which indicates the important possibility of the model to different operating characteristics of the locomotive when pulling different trains are analyzed.

In the simulations that were carried out at different contact network voltages from 19 kV to 27.5 kV. and at mechanical loads of 15 Nm and 100 Nm, almost the same results were obtained as at a voltage of 25 kV. This fact indicates an important characteristic that the locomotive drive is not sensitive to the permitted changes in the catenary voltage.

Given that the research was carried out on a model that requires input of a resisting torque on the electric motor shaft when starting the locomotive, future research will look at the influence of variable traction resistance on the traction force of the rail wheels. With additional modeling of the power transmission and axle

assembly of the locomotive, it will be possible to clearly see the output values (time changes of the firing angle of the thyristor of the single-phase rectifier, the mean voltage and current of the electric motor armature and the speed of the locomotive) at different traction resistances between the wheel and the rail.

Author contributions: Conceptualization, BG and VAB; methodology, BG; software, BG; validation, BG and VAB; formal analysis, BG; investigation, BG; resources, BG; data curation, BG; writing—original draft preparation, BG; writing—review and editing, BG; visualization, BG; supervision, BG; project administration, BG; funding acquisition, VAB. All authors have read and agreed to the published version of the manuscript.

Conflict of interest: The authors declare no conflict of interest.

References

1. Milićević Z, Arandjelović D, Marjanović V, Pejčić D. Electric locomotives JŽ 441 series. Želznid, Belgrade; 1997.
2. Dragan B. Rajković: Contribution to the analysis of axle breakage on locomotives series 441, 461 and 444. In: Proceedings of the XIV ŽELKON '10 Niš; 2010.
3. Vabić V, Grašković I. Course for service personnel of locomotive series JŽ 444 and JŽ 461-200 sedries, Končar-električne lokomotive dd., document number GO5926, archive location 211-0103. Zagreb; 2005.
4. Branislav G. Research and Analysis in the Electric Traction System of the Serbian Railways. Eliva Press; 2023.
5. Boldea I, Nasar SA. Electric Drives. CRC Press; 2016. doi: 10.1201/9781315368573
6. Nondahl, Thomas A. Microprocessor Control of Motor Drives and Power Converters, tutorial course. IEEE Industry Application Society; 1993,
7. Bolton W. Mechatronics: Electronic Control Systems in Mechanical and Electrical Engineering, 3rd ed. Pearson Education; 2004.
8. Harpreet Kaur. Electric drives and their controlling techniques. Scholar's press London; 2019.
9. Mohan N, Raju S. Analysis and Control of Electric Drives: Simulations and Laboratory Implementation. John Wiley & Sons, Inc; 2021.
10. Merabet A. Advanced Control Systems for Electric Drives. Electronics; 2021. doi: 10.3390/books978-3-03943-700-9
11. Dorji C. Review Of Electric Motor Drives. Machine Drives and control; 2015. doi: 10.13140/RG.2.1.1198.6408
12. Golnaraghi F, Kuo BC. Automatic Control Systems, 9th ed. John Wiley & Sons, Inc; 2010.
13. Kryukov OV, Blagodarov DA, Dulnev NN, et al. Intelligent Control of Electric Machine Drive Systems. In: Proceedings of the 2018 X International Conference on Electrical Power Drive Systems (ICEPDS); 2018.
14. Hughes A. Electric Motors and Drives—Fundamentals, Types and Applications, 3rd ed. Elsevier, Oxford, UK; 2006.
15. Schröder D. Elektrische Antriebe—Grundlagen, 3rd ed. Springer Berlin Heidelberg; 2007.
16. Jauch C, Tamilarasan S, Bovee K, et al. Modeling for drivability and drivability improving control of HEV. Control Engineering Practice. 2018; 70: 50-62. doi: 10.1016/j.conengprac.2017.09.014
17. Ramachandran N, Sivasubramanian R, Palanivel R, et al. Design and Fabrication of Hybrid Mobility Scooter. Advances in Materials Research; 2021.
18. Omar AMS, Samat AAA, Isa SSM, et al. New model of inverting substation for DC traction with regenerative braking system. AIP Conference Proceedings. 2017; 1875: 030016. doi: 10.1063/1.4998387
19. Barna G. Simulation model of a series DC motor for traction rail vehicles. In: Proceedings of the 21st International Conference on Methods and Models in Automation and Robotics (MMAR); 2016.
20. Wang X, Peng T, Wu P, et al. Influence of electrical part of traction transmission on dynamic characteristics of railway vehicles based on electromechanical coupling model. Scientific Reports. 2021; 11(1). doi: 10.1038/s41598-021-97650-4
21. Goolak S, Tkachenko V, Bureika G, et al. Method Of Spectral Analysis Of Traction Current Of Ac Electric Locomotives. Transport. 2021; 35(6): 658-668. doi: 10.3846/transport.2020.14242

22. Litovchenko VV, Nazarov DV, Sharov VA. Simulation Model of a Direct-Current Electric Locomotive with Commutator Traction Motors. *Russian Electrical Engineering*. 2020; 91(1): 69-76. doi: 10.3103/s1068371220010071
23. Goolak S, Saprionova S, Tkachenko V, et al. Improvement of the model of power losses in the pulsed current traction motor in an electric locomotive. *Eastern-European Journal of Enterprise Technologies*. 2020; 6(5 (108)): 38-46. doi: 10.15587/1729-4061.2020.218542
24. Chiriac G, Nituca C, Sticea D. Electric Locomotive Laboratory Test Bench for Research and Educational Purposes. 2019 8th International Conference on Modern Power Systems (MPS). Published online May 2019: 1-4. doi: 10.1109/mps.2019.8759652
25. Goolak S, Yermolenko E, Tkachenko V, et al. Determination of voltage at the rectifier installation of the electric locomotive VL-80K for each position of the controller driver's. *Technology audit and production reserves*. 2022; 1(1(63)). doi: 10.15587/2706-5448.2022.251947
26. Goolak S, Riabov I, Tkachenko V, Yeritsyan B. Simulation model of traction electric drive of AC electric locomotive equipped with collector electric motors. *Przegląd Elektrotechniczny*. 2023; 1(4): 120-129. doi: 10.15199/48.2023.04.21